by forced Rayleigh scattering and dynamic light scattering studies.[20,21] The effects of l^2 and M on R_m ($\sim N^{-4}$) prevail over that of ϕ_P^s ($\sim N^{-1}$), resulting in curve (iii) with low magnitude of R_m. Thus the homogeneous blend without appreciable composition fluctuation is expected in the ternary system consisting of very high molecular weight polymers, unless sufficient time to phase-separate is given. We think the situation is realized in Figure 11.

Concluding Remarks

We have found the development of modulated structure in solution-cast films of polymer blends. Characteristic features of the structure are the high level of phase interconnectivity and the unique periodicity. We have investigated the effects of various factors on the development of modulated structure: casting speed, polymer–polymer compatibility, blend ratio of polymers, and molecular weights of polymers. The experimental results have been interpreted in terms of the thermodynamics of ternary polymer solution and the kinetics of spinodal decomposition.

Our arguments have come from the assumption that the prevailing mechanism of phase separation during the solution casting is the spinodal decomposition. The assumption has been based on the morphological features. To verify the assumption in a quantitative sense, we should rely upon the kinetic studies of phase separation in ternary systems. The kinetic studies are under way using a temperature-drop procedure instead of the concentration jump corresponding to the solution casting. The results will be published elsewhere.[22]

Formation of the modulated structure in polymer blends has been limited to the thermally induced phase separation of the two-component polymer systems having LCST and UCST type phase diagrams.[3-5] We believe that our studies have presented a new way to prepare polymer blends with modulated structure for various polymer pairs. On the other hand, this type of study is very important in the estimation procedures of polymer–polymer compatibility, which is commonly based upon the morphological investigations and measurements of physical properties of solution-cast films of polymer blends. That is, attention should be paid to the time scale of film preparation for the proper estimation of polymer–polymer compatibility.

Acknowledgment. We acknowledge partial support by the Scientific Research Fund (Kagaku-Kenkyu-hi 58470079) of the Ministry of Education, Japan, and grants from Shinsei-shigen-kyokai, Tokyo, Japan, and the Japan Synthetic Rubber Co. Ltd., Tokyo, Japan.

Registry No. Poly(vinyl chloride) (homopolymer), 9002-86-2; poly(acrylonitrile-*co*-styrene), 9003-54-7; poly(ethylene-*co*-vinyl acetate), 24937-78-8; poly(methyl methacrylate) (homopolymer), 9011-14-7; polystyrene (homopolymer), 9003-53-6.

References and Notes

(1) Yasuda, O.; Ougizawa, T.; Inoue, T.; Miyasaka, K. *J. Polym. Sci., Polym. Lett. Ed.* **1983**, *21*, 813.
(2) Inoue, T.; Kobayashi, T.; Hashimoto, T.; Tanigami, T.; Miyasaka, K. *Polymer*, in press.
(3) McMaster, L. P. *Adv. Chem. Ser.* **1975**, *No. 142*, 43.
(4) Nishi, T.; Wang, T. T.; Kwei, T. K. *Macromolecules* **1975**, *8*, 227.
(5) Nojima, S.; Tsutsumi, K.; Nose, T. *Polym. J.* **1982**, *14*, 225.
(6) Cahn, J. W. *Trans. Metall. Soc. AIME* **1968**, *242*, 166.
(7) Hilliard, H.; Cohen, M.; Averbach, B. L. *Acta Metall.* **1961**, *9*, 536.
(8) Gardiner, J. B. *Rubber Chem. Technol.* **1970**, *43*, 370.
(9) Stein, R. S.; Rhodes, M. B. *J. Appl. Phys.* **1960**, *31*, 1873.
(10) A recent example is given by: Eastmond, G. C.; Jiang, M.; Malinconico, M. *Polymer* **1983**, *24*, 1162.
(11) Cahn, J. W. *J. Chem. Phys.* **1965**, *42*, 93.
(12) Zeman, K.; Patterson, D. *Macromolecules* **1972**, *5*, 513.
(13) Flory, P. "Principles of Polymer Chemistry"; Cornell University Press: Ithaca, NY, 1953.
(14) Scott, R. L. *J. Chem. Phys.* **1949**, *17*, 274.
(15) van Aartsen, J. J. *Eur. Polym. J.* **1970**, *6*, 919.
(16) Lodge[17] and Wesson et al.[18] have shown that the concentration dependence of the self-diffusion coefficient D_s of a polymer chain in solution is not described by a unique power law such as $D_s \sim c^{-1.75}$ (in good solvent) nor $D_s \sim c^{-3.0}$ (in Θ solvent) as described by scaling arguments (developed by de Gennes) but the slopes of log D_s–log c plots are steeper than expected, especially in concentrated solutions. Here we assumed a −4 power law only to simplify the discussion.
(17) Lodge, T. P. *Macromolecules* **1983**, *16*, 1393.
(18) Wesson, J. A.; Noh, I.; Kitano, T.; Yu, H. *Macromolecules* **1984**, *17*, 782.
(19) de Gennes, P.-G. *Macromolecules* **1976**, *9*, 594.
(20) Leger, L.; Hervet, H.; Rondelez, F. *Macromolecules* **1981**, *14*, 1732.
(21) Amis, E. J.; Han, C. C. *Polymer* **1982**, *23*, 1403.
(22) A part of the kinetic studies has been presented at the 32nd Polymer Symposium, Society of Polymer Science, Japan, Oct 1983, showing that the kinetics of phase separation can be described by the spinodal decomposition theory.

Structural Studies of Poly(*N*-vinylimidazole) Complexes by Infrared and Raman Spectroscopy

Joseph L. Lippert,* John A. Robertson, John R. Havens, and Julia S. Tan*

Eastman Kodak Company, Research Laboratories, Rochester, New York 14650.
Received December 29, 1983

ABSTRACT: Structural changes of poly(*N*-vinylimidazole) induced by metal complexation and protonation have been studied by Fourier-transform infrared and Raman spectroscopy. Ni^{2+} complexation was indicated by shifts of the imidazole ring-mode vibrational bands at 1500, 1085, and 915 cm^{-1} to higher frequencies. Spectral changes in the N–H stretching region (2400–2900 cm^{-1}) and the ring-mode deformation at 915 cm^{-1} are consistent with the formation of an H-bridged complex between the protonated and unprotonated imidazole rings upon partial protonation. These latter changes are accompanied by an intensity change in the Raman band at 1015–1020 cm^{-1}, which is suggested to be associated with a conformational change in the chain backbone.

The solution behavior of poly(*N*-vinylimidazole) has been well characterized and reported from these laboratories.[1,2] These studies show that the conformation of the polymer chain is sensitive to the degree of protonation, the degree of quaternization, the nature of the solvent, and the type of added salts. It is believed that both overall and local chain conformations of the polymer are important in its interaction with transition-metal ions and its catalytic properties.

A conformational transition of the polymer upon protonation was demonstrated by potentiometry, viscosity, and NMR studies.[2] The polymer coil first collapses upon partial protonation but expands with further protonation. The contraction of the coil during the initial stages of neutralization was interpreted as the result of H bonding between the protonated and unprotonated non-nearest-neighboring imidazole rings.

In this paper, the infrared and Raman spectroscopy of poly(*N*-vinylimidazole) is studied as a function of protonation and shown to be consistent with the existence of an H-bridged complex when partially protonated. We have also examined the Ni^{2+} complex of the polymer by vibrational spectroscopic techniques.

Experimental Section

Materials. Poly(*N*-vinylimidazole) (PVI) used in the infrared measurements was synthesized in a benzene solution[1] by Mr. W. A. Bowman and in an aqueous medium[2] by Mr. K. R. Hollister of these laboratories. No difference was observed in the infrared spectra of the polymers prepared by these two methods. PVI prepared in the aqueous medium was pale yellow and unacceptable for Raman measurements because of interferences from fluorescence. All Raman spectra reported here were obtained with PVI prepared in benzene after exhaustive dialysis.

$NiCl_2 \cdot 6H_2O$, obtained from Matheson Coleman and Bell, was used without further purification.

Methods. A. Fourier-Transform Infrared (FTIR) Spectroscopy. Infrared spectra for some of the PVI–Ni complexes were obtained from a Digilab FTS-14 infrared spectrometer with a dehumidified-air purge. Each spectrum was recorded at 2-cm^{-1} resolution and 200 scans in the range 4000–400 cm^{-1}. These measurements were made at Case Western Reserve University. Most of the FTIR spectra reported here were obtained in these laboratories with a Nicolet 7199 spectrometer at 2-cm^{-1} resolution and 64 scans. The spectra taken from the Digilab and Nicolet spectrometers were identical.

The spectra for the polymer and polymer–Ni complexes were taken in the condensed phase from sample dispersions in KBr pellets. The polymer–Ni samples were prepared by freeze-drying various stoichiometric mixtures of the polymer and Ni^{2+} solutions.

The protonated PVI samples were prepared by casting films on disks of Kodak Irtran-2 material from 2% aqueous solutions adjusted to the correct level of protonation with 1 M HCl. Solution spectra were also obtained by placing 3–8 μL of 10 wt % solutions between 2-cm-diameter Irtran disks. The volumes were adjusted so that solvent absorbances did not exceed 1.5. Solvent spectra were then subtracted in the absorbance mode, and analysis was completed on the difference spectra.

B. Raman Spectroscopy. Spectra were recorded on a Cary 82 Raman spectrometer. The samples were excited with 200 mW at 514.5 nm by a Spectra-Physics Model 164 argon ion laser. All spectra were obtained at a resolution of 9 cm^{-1} from aqueous solutions held in capillary melting-point tubes.

Results and Discussion

Poly(*N*-vinylimidazole)–Ni Complex Formation. A pale greenish blue precipitate was obtained upon addition of a PVI solution to a Ni^{2+} solution. The stoichiometry of the complex formed in a solution containing excess Ni^{2+} was [imidazole]/[Ni^{2+}] = 6/1 in aqueous solution and 4/1 in aqueous 1 M KNO_3. Quantitative studies of the complex formation constants, heats of complexation, and glass-transition temperatures of the complexes will be reported in another paper.[3]

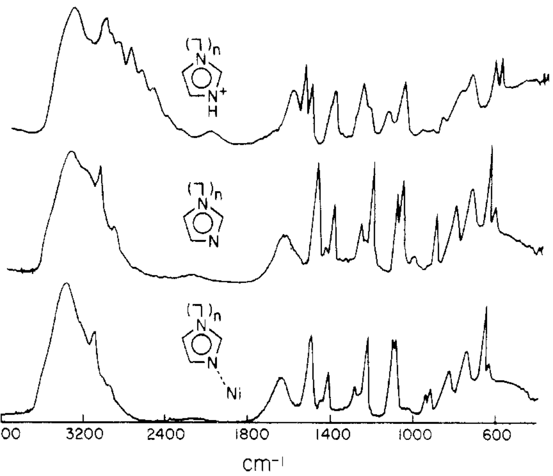

Figure 1. FTIR of the Ni^{2+} complex of PVI ($[l_T]/[M_T] = 10$), PVI, and full protonated PVI.

Table I
Vibrational Spectra of PVI and Its Protonated Form (cm^{-1})

PVI		HPVI		tentative assignments[a]
IR	Raman	IR	Raman	
3110 m		3100 m		ν CH (ring)
2950 w	2940 w	2950 w		ν CH, ν CH_2 (backbone)
		2300–2900 br, m		ν NH (protonated ring)
1500 vs	1495 sh	1573 vs		R_1 } ν C–C,C–N
1512 sh	1512 m	1544 s		R_2 } (ring)
1452 vw	1452 vw	1450		δ CH (backbone)
1350 vw	1350 vs	1450 sh	1460 s	R_3 (ν ring)
1418 m	1419 w	1430 s	1430 m	R_4 (ν ring)
1290 w	1290 m	1300 s	1310 vs	R_5 (δ CH (ring) + ν C–N (ring))
1228 vs	1233 vw	1260 m	sh	δ CH (ring) + ν C–N (ring)
		1172 m	1175 w	δ CNH (protonated ring)
1110 m	1114 w	1110 sh	1110 sh	δ CH (ring)
1085 m	1090 m	1090 m	1090 s	δ CH (ring) + ν (ring)
1020 vw	1016 m	1010 vw	1020 w	δ CH (backbone) + ν CC (backbone)
915 w	920 vw	905 w	905 w	R_6 (ν ring + δ ring)
830 sh	860 vw			R_7
820 m		830 m,br		γ CH + γ ring
745 m				γ CH + γ ring
662 vs				R_8 (ν N–C + δ ring)
638 m				γ ring

[a] ν, stretching; δ, in-plane bending; γ, out-of-plane bending.

The FTIR spectra of the neutral and fully protonated PVI and the PVI–Ni complex (6/1) are shown in Figure 1. The assignments of the peaks as listed in Table I were made in reference to those of imidazole[4,5] and *N*-methylimidazole,[6,7] with numbering of the ring modes (R_n) as described by Perchard et al.[5] On formation of the Ni^{2+} complex, the PVI ring mode (R_1) at 1500 cm^{-1} shifts to 1511 cm^{-1}, the mode at 1085 cm^{-1} (δ CH + ν ring) shifts to 1096 cm^{-1}, and the 915-cm^{-1} ring mode (R_6) decreases in intensity concurrent with the formation of a new band at 945 cm^{-1}.

The spectral changes in the 850–1150-cm^{-1} region are shown in Figure 2 as a function of $[l_T]/[M_T]$, where $[l_T]$ and $[M_T]$ are the total concentrations of the imidazole group and Ni^{2+} added. The displacements of the PVI peaks from 915 and 1085 cm^{-1} to 945 and 1096 cm^{-1}, respectively, are completed in the region $1.55 < [l_T]/[M_T] < 5.0$. This result is consistent with a stoichiometry of 4–6 determined quantitatively from binding isotherms.[3] The appearance of the polymer peaks at 915 and 1085 cm^{-1} for

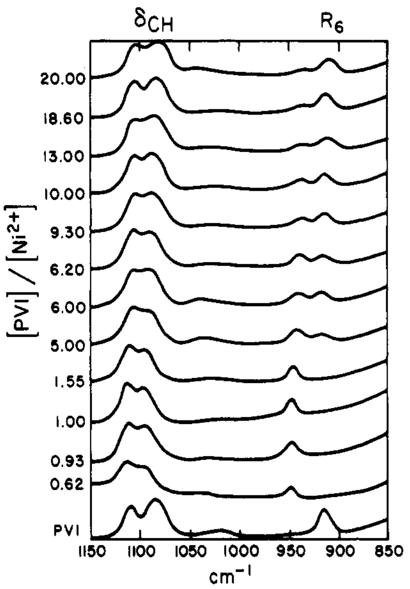

Figure 2. FTIR of the 850–1150-cm^{-1} region of PVI + Ni^{2+} at various $[l_T]/[M_T]$ ratios.

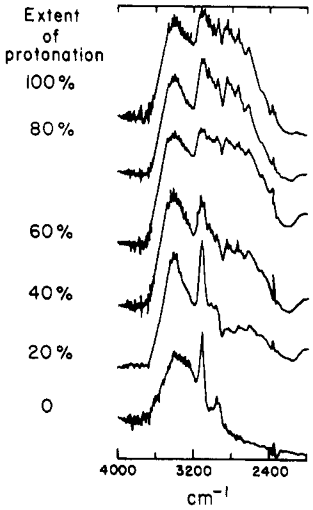

Figure 3. FTIR of the C–H and N–H stretching region of PVI films at various levels of protonation.

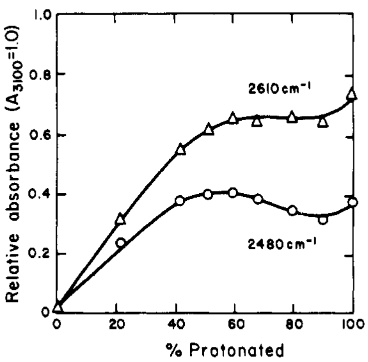

Figure 4. Plot of N–H intensities vs. extent of protonation of PVI films.

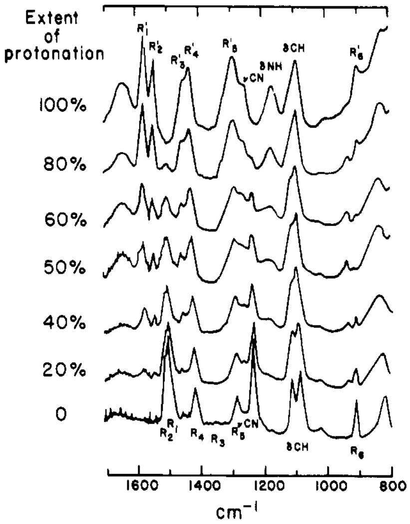

Figure 5. FTIR of partially protonated PVI films.

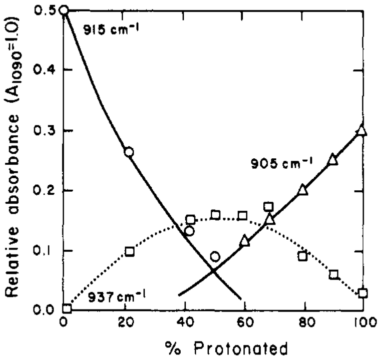

Figure 6. Plot of FTIR band intensities in the 900–950-cm^{-1} region of PVI films vs. extent of protonation.

samples with $[l_T]/[M_T] > 5$ is a result of the presence of excess uncomplexed imidazole groups.

Protonation of Poly(*N*-vinylimidazole). A. Evidence for Conformational Changes from FTIR Spectra. Infrared absorbance spectra in the C–H and N–H stretching regions of dried PVI films at various degrees of protonation (α) are shown in Figure 3. The broad peak at ca. 3450 cm^{-1} arises from the presence of a small amount of bound water in the film samples. The band structure in the N–H stretching region of the spectrum (2300–2900 cm^{-1}) is similar to that in H-bonded imidazoles and has been assigned to vibrations of different H-bonded species[8] or to Fermi resonance between the N–H stretching bands and combinations of bands in the 1000–1600-cm^{-1} region.[9,10] The latter explanation is now generally accepted.

Figure 3 shows that intensity in the N–H stretching region increases rapidly with protonation but levels off at higher α. The intensities of two of the N–H stretching bands are plotted against α in Figure 4. The initial increase in intensities would be expected as N–H bonds are formed by protonation. The occurrence of maxima at 50% protonation may be associated with the formation of an H-bridged complex between a protonated and unprotonated imidazole base pair. This H bonding could occur between adjacent or nonadjacent sites on the polymer chain or different polymer chains. The nonadjacent-neighboring H bonding is more consistent with the viscosity behavior reported earlier.[2]

Further evidence consistent with the formation of an H-bridged species is found in the mid-IR region shown in Figure 5. Tentative assignments of the vibrational spectrum of the completely protonated polymer (HPVI) are given in Table I. The HPVI spectrum contains an additional N–H band at 1172–1175 cm^{-1} (as well as the N–H stretch at 2300–2900 cm^{-1} mentioned above).

In general, spectra of partially protonated PVI contain the expected proportions of the bands associated with the PVI and HPVI species. This is evident in a plot of the intensity of such bands against α. A clear exception, however, is the band pattern at 900–950 cm^{-1}. In this region, the intensity of the R_6 ring deformation at 915 cm^{-1}

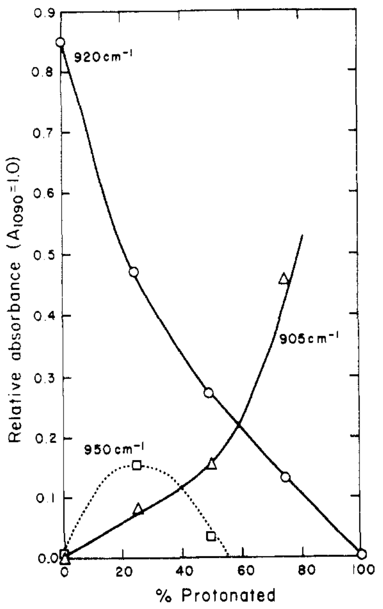

Figure 7. Plot of FTIR band intensities in the 900–950-cm^{-1} region of 10% solutions of PVI in methanol vs. extent of protonation.

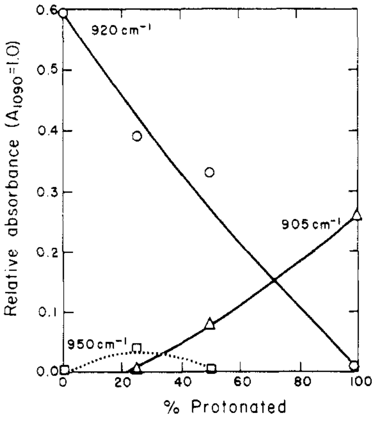

Figure 8. Plot of FTIR band intensities in the 900–950-cm^{-1} region of 10% solutions of PVI in 0.8 M aqueous NaCl vs. extent of protonation.

decreases with protonation and becomes negligible for $\alpha > 0.5$. At the same time, a band at 940 cm^{-1} reaches maximal intensity at 50% protonation and then decreases in intensity, while a band at 905 cm^{-1} (R_6 of HPVI) increases from 50% to 100% protonation (Figure 6). We believe that the band at 940 cm^{-1} may be a unique marker for imidazole–H–imidazole complex formation.

The above assignments are corroborated by those of the PVI–Ni complexes. The ring-mode vibrational bands of the uncomplexed imidazole at 1500 and 915 cm^{-1} shift to 1511 and 945 cm^{-1}, respectively, upon complexation. These spectral changes parallel those described above for the formation of an imidazole–H–imidazole complex upon protonation in dried PVI films.

To correlate the IR spectral changes associated with H-bridged complex formation in dried film and the conformational change in solutions observed previously by potentiometry, viscometry, and NMR, we examined the 900–1100-cm^{-1} region of the IR spectrum of PVI as a function of protonation in methanol and aqueous 0.8 M NaCl. The solvent spectra were subtracted from those of the solutions, as indicated in the Experimental Section. Figures 7 and 8 show the intensities as a function of α for the ring-deformation modes at 900–950 cm^{-1} in these two solvents.

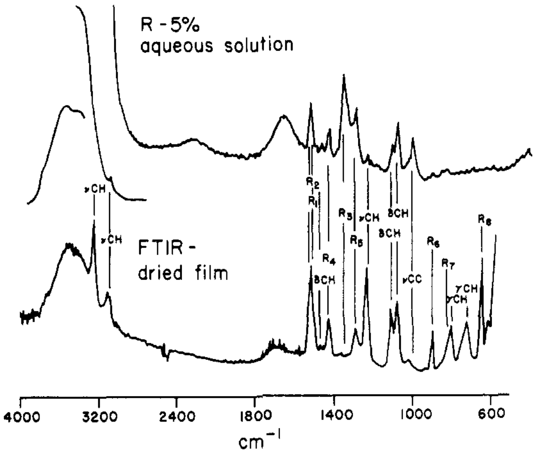

Figure 9. FTIR and Raman spectra of PVI.

In methanol, the intensity of the 950-cm^{-1} band we tentatively assign to an H-bridged complex is maximal at $\alpha = 0.3$ (Figure 7). This α value is identical with that required for minimum inherent viscosity[2] but lower than that observed above for maximum H-bond formation in dried films. This suggests that, in methanol solution, the electrostatic repulsion among the protonated sites of the polymer overrides the force for H bonding between the protonated and unprotonated base pair at a lower extent of protonation than that attained in the solid films. This would be expected, because the chloride counterions in solution are not as tightly bound to the protonated polymer sites as those in the solid state. Consequently, charge repulsion will be minimized and formation of bridged complexes will dominate in the solid state. Another possible cause for the difference in α for maximum H bonding in solution and solid films is that partial deprotonation may occur in the film sample during solvent evaporation, resulting in lower effective α than expected.

In aqueous solutions at low ionic strength, an increase in viscosity with increasing degree of protonation was observed even at low degrees of protonation.[2] At an ionic strength of 0.8 M, a shallow minimum in the viscosity curve was observed.[2] The IR data in Figure 8 show indeed that the 950-cm^{-1} complex band in high-ionic-strength aqueous solutions is reduced compared to those in methanol and dried films. One explanation for the lower stability of the complex in aqueous solutions may be the competition between water and imidazole residues for H-bonding sites.

B. Evidence for Conformational Change from Raman Spectra. Raman and FTIR spectra of the neutral PVI polymer are shown in Figure 9 for comparison. The tentative assignments of the peaks are listed in Table I. The moderately strong 1015–1020-cm^{-1} peak in the Raman, which is weak in the IR, is assigned to the C–C stretch of the polymer backbone.

Raman spectra for a series of 2% PVI solutions as a function of α in 0.88 M aqueous NaCl were recorded. A plot of the intensity of the 1020-cm^{-1} band vs. α is shown in Figure 10. A change in slope is observed at ca. 35% protonation, the same level of protonation at which the 950-cm^{-1} IR band shows a maximum (Figure 7). This suggests involvement of the backbone in a conformational change paralleling complex formation as was suggested earlier[2] on the basis of NMR studies of the same polymer. This suggestion is thus supported by the present Raman finding.

Conclusions

A. Evidence for PVI–Ni complexation was given by FTIR spectra. The ring-mode vibrations at 1500, 1085,

Macromolecules 1985, *18*, 67–78

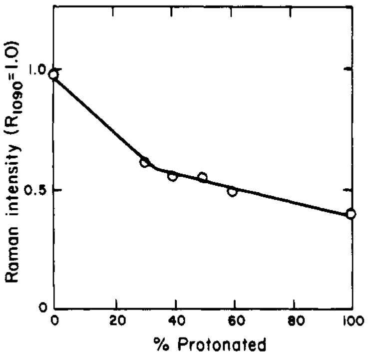

Figure 10. Plot of the relative intensity of the 1015–1020-cm^{-1} Raman band of 2% solutions of PVI in 0.88 M aqueous NaCl vs. extent of protonation.

and 915 cm^{-1} shift to 1511, 1096, and 945 cm^{-1}, respectively, upon metal incorporation.

B. The proton-bridged complex causing viscosity minima and double breaks in the potentiometric titration curves for PVI was characterized by FTIR and Raman spectra.

1. FTIR of dried films shows marker bands in the regions 2400–2600 and 900–950 cm^{-1} which appear to be associated with H bonding upon partial protonation. The band shifts in the 900–950-cm^{-1} region for protonated and Ni-complexed PVI suggest similar intrachain bridging or cross-linking in the two systems.

2. A conformational change of the backbone upon protonation is supported by the Raman spectra and is attributed to the formation of the H-bridged complexes.

Acknowledgment. We are grateful to Professor J. Koenig for discussion of some of the spectral assignments and to C. S. Baker and W. Brattlie for technical assistance.

Registry No. PVI (homopolymer), 25232-42-2.

References and Notes

(1) Tan, J. S.; Sochor, A. R. *Macromolecules* **1981**, *14*, 1700.
(2) Henrichs, P. M.; Whitlock, L. R.; Sochor, A. R.; Tan, J. S. *Macromolecules* **1980**, *13*, 1375.
(3) Handel, T. M.; Marshall, A. S.; Tan, J. S., to be submitted for publication.
(4) Cordes, M.; Walter, J. L. *Spectrochim. Acta, Part A* **1968**, *24a*, 237.
(5) Perchard, C.; Bellocq, A. M.; Novak, A. *J. Chim. Phys. Phys.-Chim. Biol.* **1965**, *62*, 1344.
(6) Perchard, C.; Novak, A. *Spectrochim. Acta, Part A* **1967**, *23a*, 1953.
(7) Sheinker, V. N.; Movshovich, D. Y.; Osipov, O. A.; Garnovskii, A. D. *Zh. Obshch. Khim.* **1973**, *43*, 2725.
(8) Zimmerman, H. *Z. Electrochem.* **1961**, *65*, 821.
(9) Wolff, H.; Wolff, E. *Spectrochim. Acta, Part A* **1971**, *27a*, 2109.
(10) Wolff, H.; Muller, H. *J. Chem. Phys.* **1974**, *60*, 2938.

SANS and SAXS Studies on Molecular Conformation of a Block Polymer in Microdomain Space

Hirokazu Hasegawa, Takeji Hashimoto,* and Hiromichi Kawai[†]

Department of Polymer Chemistry, Kyoto University, Kyoto 606, Japan

Timothy P. Lodge,[‡] **Eric J. Amis,**[§] **Charles J. Glinka, and Charles C. Han***

Center for Materials Science, National Measurement Laboratory, National Bureau of Standards, Washington, D.C. 20234. *Received March 26, 1984*

ABSTRACT: The molecular conformation of a block polymer chain in a microphase-separated domain space (a confined space) was studied by small-angle neutron scattering (SANS) with a deuterium labeling technique. The samples studied were polystyrene–polyisoprene diblock polymers, and they have a morphology of highly oriented alternating lamellar microdomains composed of polystyrene (PS) and polyisoprene (PI) in bulk when cast from dilute solutions in toluene. Small-angle X-ray scattering (SAXS) measurements were conducted on the same specimens used for SANS in order to separate the scattering arising from a single chain $P(q)$ and that arising from the microdomain structure $S(q)$. Components of the radius of gyration of the single deuterated PS chain in PS lamellae, parallel (R_{gx} or R_{gy}) or perpendicular (R_{gz}) to the interfaces between the two microdomains, were determined with the high-concentration labeling technique of SANS coupled with the SAXS technique. The results indicated that (i) the chain is expanded normal to the interfaces, giving rise to $R_{gz} \simeq 1.6R_{gx}$, (ii) the chain is contracted parallel to the interfaces, giving rise to $R_{gx} \simeq 0.7R_{gx,0}$ ($R_{gx,0}$ being a component of the radius of gyration of the corresponding unperturbed chain), and (iii) the longitudinal expansion is compensated by the lateral contraction, giving rise to an overall radius of gyration R_g nearly equal to or slightly less than R_{g0} for the unperturbed chain. Conclusion (iii) does not mean at all that the chains in domain space are unperturbed but rather that they are strongly perturbed. The lateral contraction was proposed to be the consequence of the repulsive potential between the centers of block chains which are located in narrow interfacial regions (i.e., essentially in the two-dimensional space). A residual "memory" of the repulsion in the bulk block polymer could be a consequence of the two-dimensionality of the space available to chemical junctions of the block polymers and/or an effect of repulsive potential (which existed in the polymer solution with a good solvent) being "locked-in" at high polymer concentrations.

I. Introduction

It is well-known that block polymers (e.g., AB) adopt a microdomain structure in the strong segregation regime for which $\chi Z \gg (\chi Z)_c$, where χ is the Flory–Huggins interaction parameter between the constituent polymers A and B, Z is the total degree of polymerization of the AB diblock polymer, and $(\chi Z)_c$ is the critical value of χ.[1-15] In this regime, A (B) polymers segregate themselves into A (B) microdomains with their chemical junction points being localized in narrow interfacial regions (Figure 1).[3,9,10,13,14,16-25] The "characteristic interfacial thickness"[9] is reported to be about equal to or less than 2 nm for polystyrene–polyisoprene (SI) or polystyrene–poly-

---

[†] Current address: Hyogo University of Education, Yashiro-cho, Kato-gun, Hyogo-Ken, Japan.

[‡] Current address: Department of Chemistry, University of Minnesota, Minneapolis, MN 55455.

[§] Current address: Department of Chemistry, University of Wisconsin, Madison, WI 53706.

0024-9297/85/2218-0067$01.50/0